A multi-lattice sampling approach for highly undersampled phase contrast carotid blood velocity mapping

Gabriel Rilling[1], Yuehui Tao[2], Mike E. Davies[1], and Ian Marshall[2]

[1]School of Engineering, University of Edinburgh, Edinburgh, Scotland, United Kingdom, [2]Medical Physics, University of Edinburgh

1. Introduction

Common undersampling strategies for dynamic MRI with Cartesian trajectories are either based on lattice or random sampling in (k,t) space. Lattice sampling is the basis of methods such as UNFOLD [1] or ktBLAST [2]. Random sampling is associated with methods based on the compressed sensing theory, such as ktSPARSE [3] or ktFOCUSS [4]. Lattice sampling offers maximal acceleration and robustness to noise if the (y,f) support (2D Fourier domain of (k,t)) of the signal can be tiled by the 2D Fourier transform of the (k,t) sampling pattern. This implies strong constraints on the sampling lattice which limit the achievable acceleration. In contrast, random sampling patterns can be designed independently of the support shape but offer poorer robustness to noise compared to lattice sampling. The multi-lattice approach we propose is intermediate between lattice and random sampling, with the goal of providing more flexibility than lattice sampling and better noise robustness than random sampling.

2. Phase contrast carotid blood velocity mapping and signal support

Complex-valued raw signal of a single axial carotid slice (192×192 image with 24 time frames, Fig. 1) was collected on a GE 1.5T Signa HDx scanner (GE Healthcare, Slough, UK) in 2D phase contrast carotid acquisition of a healthy volunteer. Time frames were collected in each retrospective gated acquisition. Velocity encoding was applied only in the S/I direction. Inverse Fourier transform was applied in the frequency-encoding dimension to allow separate processing of data at each L/R location (x). For a typical (y,t) slice at a given x going through the left common carotid artery (LCCA), the image is essentially static except inside the LCCA. The signal support in the (y,f) domain can thus be modelled as in Fig. 2.

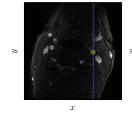## 3. Multi-lattice sampling for mutli-block supports

The signal support can be viewed as the combination of two blocks: a static block with only DC frequency content which occupies (almost) all the space in the y direction and a dynamic block that is localized in a small region corresponding to the LCCA. Each of these blocks has a rectangular shape and can therefore be individually optimally sampled using lattice sampling. We propose to use a multi-lattice sampling pattern designed as a combination of lattices adapted to each block shape. The multi-lattice pattern can be further optimized by an exhaustive search through all combinations of two lattices adapted to the two support block shapes. Such a multi-lattice pattern allows the reconstruction of any signal whose support is composed of two blocks with these shapes, whatever their locations. In practice, this implies that the location of the LCCA does not need to be known a priori to design the sampling pattern. However, it needs to be known for the reconstruction.

4. Detection of the common carotid arteries and signal reconstruction

By averaging multi-lattice (k,t) samples over t, estimates of the static images are first reconstructed for both the velocity encoded and non-velocity encoded image series. Voxels with non-zero velocity on average are then characterized by different phases between the two static images. This allows us to efficiently detect the carotid arteries as circular regions in the static images exhibiting at the same time a rather large magnitude and a phase difference indicating velocity towards the head. Given the location of the arteries, the location of the dynamic block in the (y,f) support is known and the coefficients on the support can be reconstructed using a regularized least squares approach, similar to the ktBLAST reconstruction formula. For this reconstruction, the diagonal of the signal covariance matrix can be estimated based on the static images and a sensible a priori frequency profile for the dynamic block.

5. Simulations and in vivo experiments

Using a combination of two lattices as described previously leads to a 8× acceleration factor. However, the high spatial frequencies are mostly static for this application which allows us to use a ``keyhole'' [5] approach and only sample the center half of k-space for the dynamic lattice, and in turn increase the acceleration to 12× (see Fig. 3, (a)+(b)). However, at such a high acceleration factor, any measurement noise may cause a rather poor SNR. The SNR can be improved by adding more measurements, for instance by doubling the number of samples in the dynamic lattice, leading to a 8× acceleration sampling pattern (see Fig. 3, (a)+(c)). These 12× and 8× acceleration patterns have been simulated from images reconstructed from a fully sampled scan. The 8× pattern has also been implemented in vivo, immediately after the acquisition of the fully sampled scan. The simulation results show a reasonably good performance of the 12× acceleration pattern, which is slightly improved by the additional samples in the 8× pattern (see Fig. 4). Quantitatively, the RMS velocity errors across the artery for 12× and 8× are 6.4 cm/s and 5.3 cm/s respectively. The performance of the 8× pattern in vivo is not as good, but still acceptable with a 5.9 cm/s RMS error.
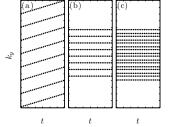

Figure 1: Axial carotid slice with the LCCA marked in yellow. An x location going through the LCCA is marked in blue.

Figure 2: Signal model: static block (dark gray) and dynamic block (light gray).

Figure 3: Sampling patterns for 12× (patterns (a)+(b)) and 8× (patterns (a)+(c)) acceleration.
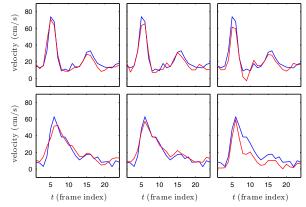
Figure 4: Velocity estimation (red) and reference (blue) for two representative voxels. Top row: voxel in the center of the LCCA. Bottom row: voxel close to the artery wall. From left to right: 12× (simulation), 8× (simulation) and 8× (in vivo).

References

[1] Madore, B. *et al.*, Magn Reson Med. 42, 813–828 (1999)
[2] Tsao, J. *et al.*, Magn. Reson. Med. 50, 1031–1042 (2003)
[3] Lustig, M. *et al.*, ISMRM'06 (2006)
[4] Jung, H. *et al.*, Phys. Med. Biol. 52, 3201–3226 (2007)
[5] Van Vaals, *et al.*, J. Magn. Reson. Imag. 3, 671–675 (1993)